

Characterization and corrosion properties of electrodeposited Ni-W alloys*

M. OBRADOVIĆ^{1#}, J. STEVANOVIĆ^{1#+}, A. DESPIĆ^{1#}, R. STEVANOVIĆ^{1#} and J. STOCH²

¹*ICTM - Institute of Electrochemistry, Njegoševa 12, P. O. Box 473, YU-11001 Belgrade, Yugoslavia and* ²*Institute of Catalysis and Surface Chemistry, Polish Academy of Sciences, Niezapominajek 1 30-239 Krakow, Poland*

(Received 30 July, revised 8 August 2001)

Ni-W alloys electrodeposited from citrate solution consist of three different phases, which are all present in high W-content alloys: a solid solution of W in a Ni matrix; an intermetallic compound Ni₄W, as well as another solid solution of W in Ni with a W content higher than 20 mol. %. XPS analysis revealed that the alloys were covered with a surface layer of complex structure containing the pure metals Ni and W, Ni(OH)₂ and WO₃, on the very surface as well as some partially reduced oxide WO_{2.72} (most probably a solid solution of WO_{2.72} in Ni) and tungsten carbide in the layer underneath. It is highly likely that some of the oxide species in the layer act as intermediates in the cathodic deposition process. Identifying these species should be the clue to a more detailed understanding of the mechanism of induced deposition of W than has been achieved so far. Corrosion of Ni-W alloys in sulfuric acid solution at OCP, occurs by the preferential dissolution of nickel from the surface layer. The longer the corrosion process lasts, the more the surface behaves like pure W. The lowest initial corrosion rates were recorded with alloys rich in W, but after aging at OCP the lowest corrosion c.d. was found for the Ni-W alloy with the most homogenous phase structure, consisting of the solid solution only.

Keywords: nickel-tungsten, induced codeposition, phase structure, corrosion.

INTRODUCTION

The interest in electrodeposited alloys of tungsten and molybdenum with iron group metals is due to their specific magnetic, electrical, mechanical, thermal and corrosion properties.^{1,2} In recent years, these alloys and particularly their composites as well as their compositionally modulated multilayers³ met the enhanced need of modern industry for materials with specially designed properties. For their practical use, it is essential to learn about their corrosion properties. Hence, some authors devoted their work to this subject, as well.

* Dedicated to Professor Dragutin M. Dražić on the occasion of his 70th birthday.

Serbian Chemical Society active member.

+ Corresponding author: e-mail: rade@elab.tmf.bg.ac.yu

Thus, Atanasov *et al.*³ found for example, that the corrosion of a Ni-W alloy, obtained from a sulfamate bath, in H₂SO₄ (0.5 mol dm⁻³), leads to the dissolution of Ni and an enrichment in W by about 10 %. In 3 % NaCl, contrary to expectations, the corrosion resistance is increased and elution of Ni is decreased. They also found that the corrosion is affected by the phase composition, morphology and grain size of the deposit. To improve the morphology, Donten and Stojek⁴ used pulse plating and claimed that an increased resistance to corrosion resulted. They found this to be the result of the elimination of the uneven composition of the alloy constituents at the surface, some of which have up to 10 % lower W content than the average.

As could be expected, the general conclusion from the previous work is that the corrosion behavior of these alloys is very complex, depending on the W content, on the structure of the alloy and on the corrosion medium, but also on the component from the Fe-group of metals. Thus, the corrosion resistance appears to increase in the order Fe-Ni-Co.^{1,2} However, few details are available on the subject. No study was found in which an attempt was made to relate directly the corrosion properties to the chemical composition and phase structure of electrochemically obtained deposits. It was the aim of this work to obtain a better insight into this relationship.

The composition and structure of Ni-W alloys are sensitive to the composition of the electrolyte from which they were deposited, to the pH in particular, as well as to the current density (c.d.) and hydrodynamic conditions of the deposition. Hence, the influence of each of these was examined in a previous paper.⁵ In the present communication, the conditions of deposition were selected so as to produce alloys with distinctly different phase compositions and to investigate the effects of the composition on their corrosion properties. The main method used in the analysis of the deposits was that of anodic linear sweep voltammetry (ALSV), which was proven to be a good tool for phase characterization.⁶

EXPERIMENTAL

Ni-W alloys were electrodeposited from two baths recommended in the plating literature.⁷ They were: a) an ammonia-citrate bath containing NiSO₄ (0.075 and 0.110 mol dm⁻³), Na₂WO₄ (0.2 mol dm⁻³), citric acid (0.3 mol dm⁻³), where the pH of 8.15 was adjusted by the addition of NH₃, and b) a citrate-borate bath containing 0.93 mol dm⁻³ NiSO₄, 0.088 mol dm⁻³ NiCl₂, 0.060 mol dm⁻³ Na₂WO₄, 0.68 mol dm⁻³ trisodium citrate, 0.50 mol dm⁻³ H₃BO₃, 0.27 mol dm⁻³ KCl, 0.93 mol dm⁻³ NH₄Cl. All the chemicals were of reagent grade quality and were dissolved in triply distilled (18 MΩ) water.

The working electrode was an Au disc (0.26 cm² surface area), which could be rotated (RDE) by a Tacussel-Controvit rotating assembly.

A conventional glass electrochemical cell was used with a SCE reference electrode, a Pt-counter electrode in a separate compartment and with provisions for thermostating and purging the electrolyte free of oxygen by purified nitrogen. Hence, all the potentials are referred to the SCE.

Deposition was carried out without rotation and at rotation rates of 250 and 1000 rpm, as well as at different constant temperatures of 25, 35 and 55 °C. The alloys were deposited galvanostatically, at 50 and 100 mA cm⁻², to a constant total quantity of electricity of 4, 10 and 50 C cm⁻² using a PAR 273 potentiostat/galvanostat.

The Ni and W contents of the metallic deposits were determined by EDS (Energy Dispersive Spectroscopy), while their surface was examined by XPS (X-ray Photoelectron Spectroscopy).

The phase-compositions were investigated by X-ray diffraction and by anodic linear sweep voltammetry (ALSV). In order to avoid passivation, the anodic linear sweep dissolution was carried out in an electrolyte containing 1 mol dm^{-3} NaCl and 0.01 mol dm^{-3} HCl to which the samples plated on the RDE were transferred upon deposition. The scan rate in the ALSV was very low (0.1 mV s^{-1}) and was carried out in a potential range necessary for complete dissolution. The ALSV experiments were performed at room temperature.

The recorded voltammograms were integrated to establish the equivalent quantity of electricity obtained upon dissolution. These data were used for calculating the current efficiency of deposition.

In order to estimate the influence of the phase composition on the corrosion properties, galvanostatic steady-state cathodic and anodic polarization curves for Ni-W alloys, pure Ni deposit and W wire were recorded in acid solution (0.5 mol dm^{-3} H_2SO_4) around the open circuit potential, OCP, and before the passivity region. In the wider anodic potential range, a potential sweep rate of 0.3 mV s^{-1} was used. Care was taken that before the polarization measurements were made, a constant OCP was always established. It took up to 120 min prior to the measurements for the OCP to stabilize and subsequently one minute of recording was given to each point. Within the employed anodic current density range, the anodic polarization could not change the deposit substantially.

RESULTS

Chemical composition and phase structure of the alloys

The alloys investigated in this work were deposited under the conditions specified in Table I. The ALSV voltammograms were found to exhibit peaks dependent on the conditions of deposition. They were deconvoluted and integrated to render the quantities of electricity spent on the deposition of the individual phases.

TABLE I. Deposition conditions, current efficiency of the Ni-W deposition, W content in the alloy and fractions of the total ALSV charge pertaining to a particular ALSV peak.

Sample	Deposition conditions						η_I	$x(\text{W})$	$x(\text{I})$	$x(\text{II})$	$x(\text{III})$	$x(\text{IV})$
	j_{dep} mA cm^{-2}	t_{dep} $^\circ\text{C}$	ω_{dep} rpm	Q_{dep} C cm^{-2}	$c(\text{Ni})$ mol dm^{-3}							
1	50	25	1000	4	0.075	0.32	0.19	0.18	0.59	0.187	0.04	
2	50	25	1000	10	0.075	0.34	0.19	0.07	0.53	0.308	0.10	
3	50	35	0.0*	4	0.075	0.40	0.14	0.17	0.64	–	0.19	
4	100	25	1000	4	0.075	0.28	–	0.29	0.65	–	0.05	
5	50	25	1000	4	0.110	0.35	–	0.37	0.53	–	0.11	
6	50	25	250	4	0.075	0.31	0.10	0.41	0.53	–	0.06	
7	50	25	0.0*	4	0.075	0.31	0.10	0.41	0.49	–	0.10	
8**	50	55	0.0*	4	1.02	0.72	0.03	–	1.0	–	–	

*natural convection, vertical electrode; **citrate-borate bath

Typical ALSV responses of Ni-W alloy layers deposited galvanostatically in the citrate-ammonia bath to a quantity of electricity of 4 C cm^{-2} , at a rotation rate 1000 rpm (sample 1) and with a stationary electrode (sample 7), are given in Fig. 1 (a and b, respectively).

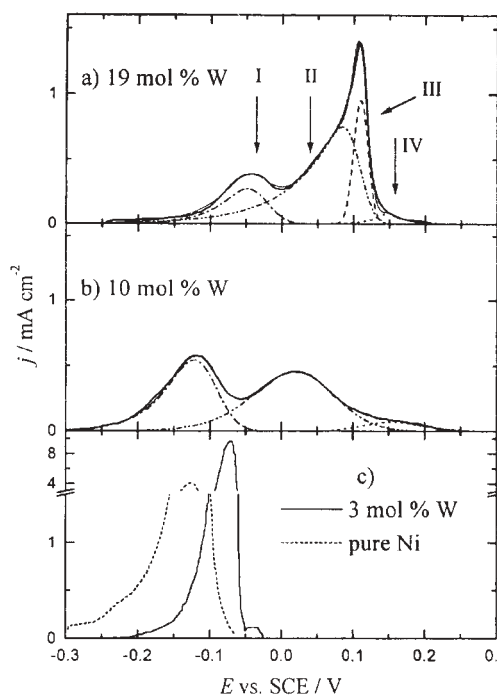


Fig. 1. Typical ALSV responses for the dissolution of Ni-W layers deposited galvanostatically at 50 mA cm^{-2} ; citrate-ammonia (a and b) and citrate-borate bath (c); rotating rate $\omega = 1000 \text{ rpm}$ (a and c) and at a stationary electrode (b); temperature $25 \text{ }^\circ\text{C}$ (a and b) and $55 \text{ }^\circ\text{C}$ (c); ALSV sweep rate 0.1 mV s^{-1} , solution $0.1 \text{ mol dm}^{-3} \text{ NaCl} + 0.01 \text{ mol dm}^{-3} \text{ HCl}$.

The oxidation of the alloys deposited when the rotation rate was 1000 rpm in all cases took place at more positive potentials than that of pure nickel and, in general ALSV, consisted of up to four peaks reflecting the presence of different structures. The first peak (peak I) was found in the interval between -0.13 and -0.05 V and peak II appeared in the interval between 0.00 and 0.08 V . A sharp peak III with a maximum at a potential around 0.11 V and a small peak IV around 0.150 V were also recorded.

Deposition under the same conditions but without rotation of the electrode rendered an ALSV with only two peaks (Fig. 1b), with peak potentials shifted in the negative direction compared with corresponding peaks in the case of a rotating electrode.

In order to obtain an alloy with a low W content, deposition from a citrate-borate bath was also carried out (*cf.* experimental). In this case, the alloy was deposited to the same quantity of electricity, onto a stationary electrode at $55 \text{ }^\circ\text{C}$ (sample 8). The ALSV of this alloy is given in Fig. 1c. It proved to be similar to that obtained for pure Ni, deposited in the absence of tungstate in the solution, but with a peak potential shifted by about 0.06 V in the positive direction.

Current efficiencies of deposition, η_{dep} , as well as the relative amounts of the different phases are also shown in Table I.

According to XPS measurements, Ni is present at the surface of the alloy in the metallic state (Binding energy, $BE = 852.6 \text{ eV}$) and as hydroxide $\text{Ni}(\text{OH})_2$ ($BE = 853.8$

–854.6 eV), while W is present as metallic ($BE = 31.5$ eV) and as oxide WO_3 on the top of it ($BE = 35.8$ eV). After ion etching of the surface, partially reduced W oxides are found (mainly $WO_{2.72}$, $BE = 34.8$ eV) instead of WO_3 . After etching, the presence of significant amounts of carbon in the deposits was found through some contribution of a C1s band. The W content in all the deposited alloys was in the range between 3 mol % (Fig. 1c) and 19 mol % (Fig. 1a). X-ray diffraction did not reveal any pattern, implying that the crystals in the deposits were very small, falling beyond the Bragg's limit.

Influence of phase composition on the corrosion properties of the alloy layers

The polarization behavior of pure Ni and W wire were recorded in order to learn about the corrosion properties of the pure metals, for comparison with the behavior of the deposited alloys, under the same conditions. The samples were held at the OCP prior to polarization, except for pure Ni, which was held for only 20 min because of alteration of the surface of the deposit at the high corrosion rate. Complex $E - \log j$ relations were obtained, as presented in Fig. 2.

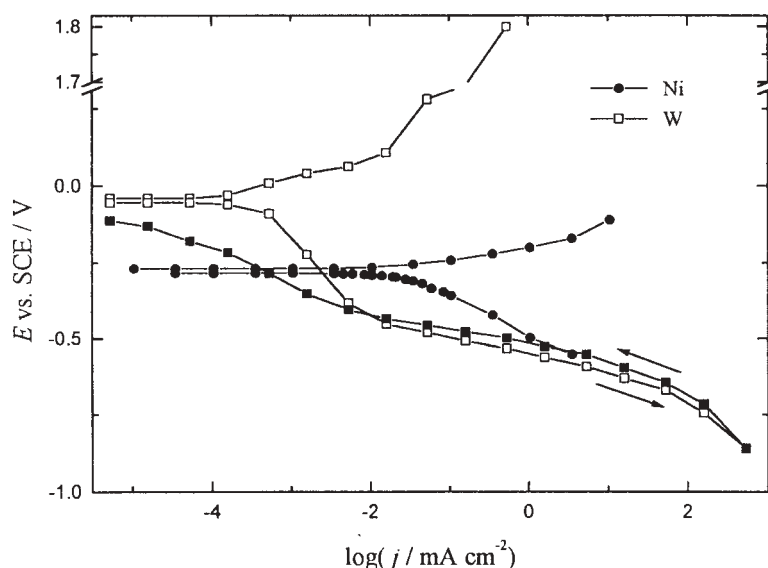


Fig. 2. Galvanostatic polarization of the pure metals, Ni and W, in $0.5 \text{ mol dm}^{-3} \text{ H}_2\text{SO}_4$ solution.

For pure Ni, an OCP of -0.269 V vs. SCE and linear parts of anodic and cathodic Tafel plots with slopes of $b_a = 30 - 40 \text{ mV dec}^{-1}$ and $b_c \cong -120 \text{ mV dec}^{-1}$, respectively, were obtained.

The $E - \log j$ dependencies for pure W in H_2SO_4 solution exhibited several features: i) the OCP was -0.050 V vs. SCE ; ii) at low cathodic overpotentials, a limiting current of approximately $3 \mu\text{A cm}^{-2}$ was found; iii) at cathodic potentials more negative than about -0.300 V , a linear Tafel line with a slope close to -60 mV dec^{-1} was obtained. In the reverse direction, from high c.ds back the limiting current was less pronounced. In the anodic region, a Tafel line with a slope of 60 mV dec^{-1} was obtained.

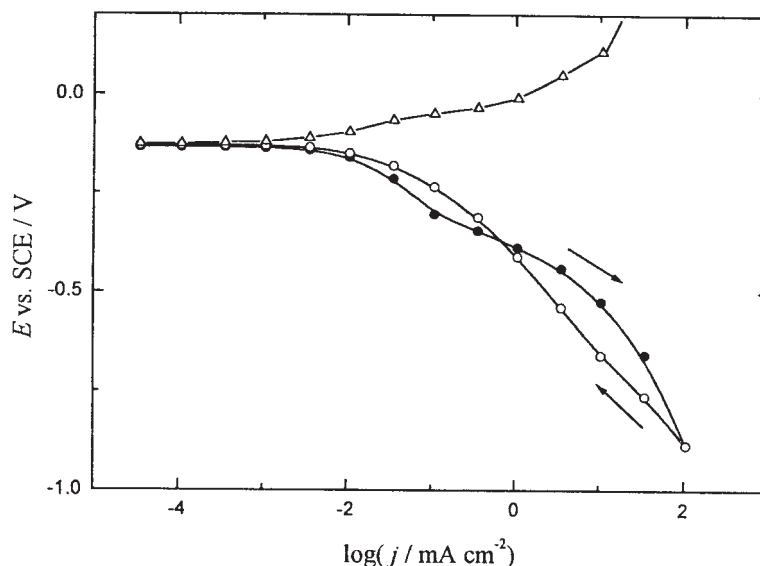


Fig. 3. Galvanostatic polarization of the Ni-W alloy characterized by the ALSV of Fig. 1a, in $0.5 \text{ mol dm}^{-3} \text{ H}_2\text{SO}_4$ solution.

Galvanostatic anodic and cathodic polarization curves for a typical alloy (the one characterized by the ALSV of Fig. 1a) were recorded in the forward as well as in the reverse direction (Fig. 3). After immersion into $0.5 \text{ mol dm}^{-3} \text{ H}_2\text{SO}_4$, the OCP of the alloy changes in the negative direction from 0.25 V vs. SCE , to -0.13 V vs. SCE after 120 min. Upon cathodic polarization an apparent limiting c.d. of about $30 \mu\text{A cm}^{-2}$ is reached in the interval between the OCP of the alloy and the theoretical reversible potential of hydrogen (-0.27 V vs. SCE). After reaching the highest c.d., 100 mA cm^{-2} , upon reversing the direction, at potentials more negative than about -0.35 V vs. SCE , a linear Tafel plot with a slope of -200 mV dec^{-1} was recorded. It should be noted that at these relatively high c.ds, polarization in the reverse direction leads to a higher overvoltage than in the direction of increasing c.d. Repetitive measurements in both directions reproduced quite well the shape of the cathodic polarization curves. They were both reproduced even after application of 350 mA cm^{-2} during 20 min, *i.e.*, no reduction of the surface took place. The only change was that the OCP became somewhat more negative than before.

Anodic polarization is characterized by an abrupt rise in the polarization at c.ds, higher than 10 mA cm^{-2} , which indicates passivation of the surface. A sudden polarization increase has been recorded for other alloy specimens as well.

Corrosion currents, j_{COR} , could not be determined using the inflection point method⁸ since uncommon values of the Tafel slopes for the cathodic process were obtained. Hence, the corrosion c.ds had to be estimated from the intersections of the anodic Tafel plots with the OCP.

The corrosion potentials and corresponding corrosion currents for pure metals as well as for the alloy samples of Table I, are all given in Table II. It can be seen that the es-

timated corrosion current for Ni is about 240 times larger than that for W and two to ten times larger than those pertaining to the alloys of different composition.

TABLE II. Corrosion parameters of electrodeposited Ni-W layers as function of the W content of the alloy*

Sample	$x(\text{W})$	$-E_{\text{OCP}}/\text{V}$	$j_{\text{cor}}/\mu\text{A cm}^{-2}$	$j_{\text{cor}}'/\mu\text{A cm}^{-2}$
W	1.00	0.05	0.1	0.3
1	0.19	0.127	2.5	16
3	0.14	0.145	4.3	23
6	0.10	0.220	3.3	37
8	0.03	0.260	10	52
Ni	0.00	0.274	24	82

* Corrosion current densities, j_{cor} , were extracted from the galvanostatic polarization measurements, taken after 120 min of stabilization at OCP, while j_{cor}' were extracted from the set of passivation experiments, performed immediately after immersion into the solution.

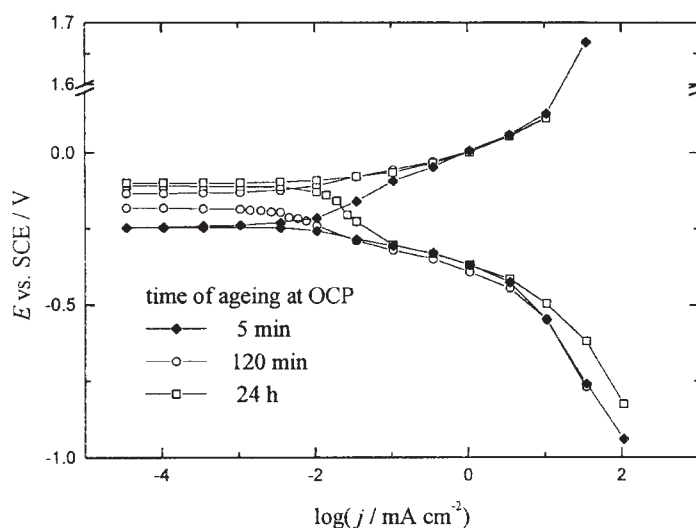


Fig. 4. Galvanostatic polarization dependencies of a Ni-W alloy (sample 2 in Table I) obtained after different times of ageing at OCP, solution $0.5 \text{ mol dm}^{-3} \text{ H}_2\text{SO}_4$.

In addition, some thicker alloy specimens (typically sample 2 in Table I) were left to rest at open circuit for different periods of time. After 5 min, 120 min and 24 h of ageing, polarization measurements were performed and the obtained cathodic Tafel plots are shown in Fig. 4. It should be noted that ageing at the corrosion potential leads to some depolarization effect at higher cathodic c.ds. It can be seen that the longer the period of ageing, the more positive the OCP value, closer to that pertaining to pure W. Simultaneously, the limiting cathodic current becomes more pronounced and the corrosion c.d. somewhat increased.

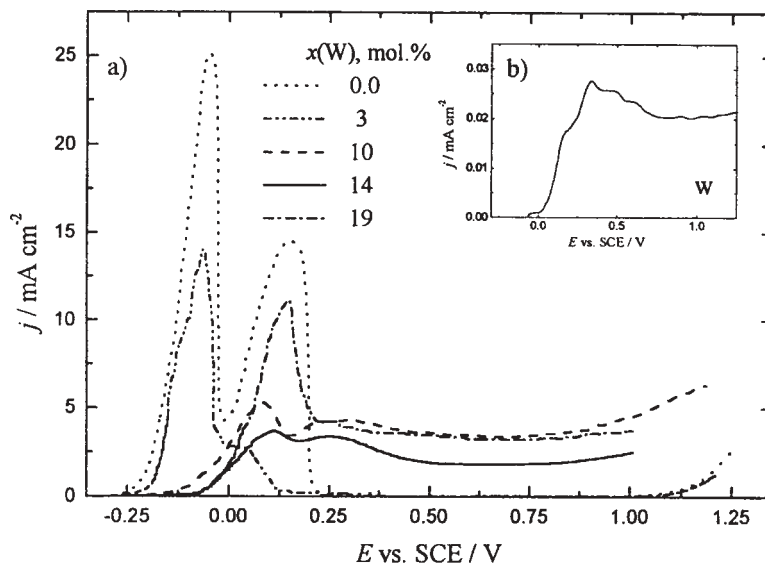


Fig. 5. Anodic quasipotentiostatic polarization of pure Ni and Ni-W alloys of different W content (a) as well as of pure W (b); ($v = 0.3 \text{ mV s}^{-1}$), solution $0.5 \text{ mol dm}^{-3} \text{ H}_2\text{SO}_4$.

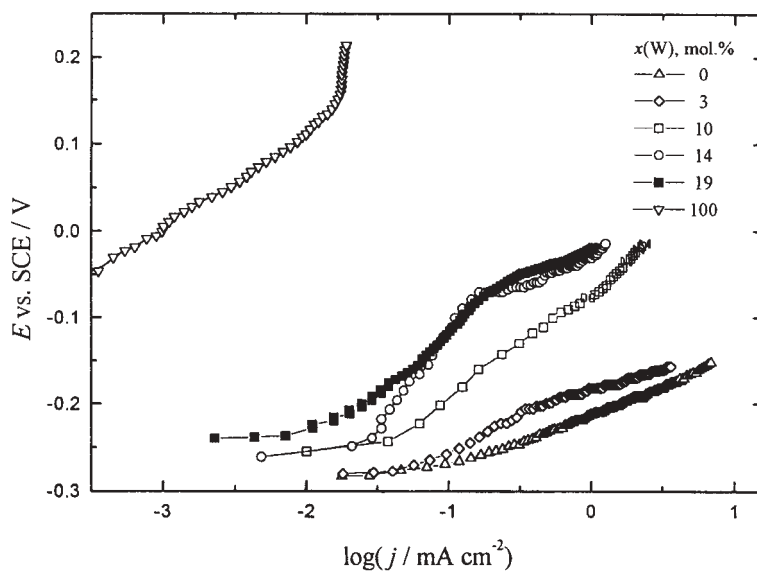


Fig. 6. Initial portions of the polarization dependencies of Fig. 5, on the log scale.

Contrary to this, the time of ageing at the corrosion potential does not affect the anodic polarization curves at c.ds higher than about 3.5 mA cm^{-2} , where they all virtually overlap.

In order to obtain more insight into the passivation process, anodic quasipotentiostatic (0.3 mV s^{-1}) polarization curves were also recorded. It can be seen in Fig. 5

that pure Ni and the alloy with minimal content of W both dissolve actively upon the start of anodic polarization from their corrosion potentials. After a peak at a potential of -0.065 V vs. SCE, passivation occurs. After the passivation potential of 0.20 V vs. SCE is reached a c.d. of $20 \mu\text{A cm}^{-2}$ is maintained throughout the entire passive region up to 1 V vs. SCE. It should be noted that Ni dissolves with two peaks, while the alloy exhibits only a potential arrest at 0.00 V vs. SCE.

With the other alloys, containing more W and with dissolution peaks at more positive potentials, the situation is somewhat different. The dissolution starts from significantly more positive potentials, but passivation is not effective. After a peak at about 0.150 V vs. SCE, which coincides with the second peak of Ni, relatively large dissolution currents of the order of 1 mA cm^{-2} persist up to the positive potential limit of 1 V.

The initial parts of the passivation curves of Fig. 5 up to the peak potentials are given on the logarithmic scale in Fig. 6. Corrosion c.ds were again estimated from the intersections of the anodic Tafel plots with the OCP. The alloys exhibit corrosion c.ds in the range between those of Ni and W. Also, the larger the Ni content, the larger are the corrosion c.ds, approaching that of pure Ni (*cf.* Table II, j_{cor}).

DISCUSSION

Structure of the alloy deposits

All the alloys with a relatively large W content (above 15 %) render ALSV with several peaks at potentials significantly more positive than that of Ni dissolution, as is shown in Fig. 1a.

The first peak suggests the existence of a surface layer of constant thickness, on top of the bulk of the deposit. This could be concluded from the fact that alloy samples 1 and 2, which were deposited under the same conditions, but with different quantities of electricity, rendered ALSVs containing one and the same quantity of electricity under peak I. This implies that some layer on the top of the alloy deposit could be grown to a limited extent only.

When considering possibilities of investigating the structure of this layer, it should be noted that a suitable method is XPS, in that the results it renders are related to species in the surface layer only and not to those in the bulk of the alloy. The composition found by measurements before etching corresponds to species on the very surface while those found after etching pertain to species somewhat deeper, yet still in the surface layer. The XPS investigations revealed that the very surface layer, facing the solution, appears to be a mixture containing Ni, W, Ni(OH)_2 and WO_3 , indicating heterogeneity in the surface morphology, possibly with grains of different composition. Also, underneath the very surface, $\text{WO}_{2.72}$ and some carbon were found. The $\text{WO}_{2.72}$ can be considered as a mixture of WO_3 with oxides of valences lower than 6. In fact, oxide structures having higher valency oxides at the top near the oxide/solution interface and lower valency oxides near the metal/oxide interface are not uncommon for most metals covered by oxide films. The oxidation capacity of that phase is due to Ni species, but also to some lower oxide of W constituting $\text{WO}_{2.72}$.

The carbon 1s band suggests the presence of tungsten carbide, found also by Dönten *et al.*⁹ in Co-W deposits. The presence of carbon incorporated in that form, rather than as the pure element (graphite), can explain the significant hardness of these alloys when deposited from citrate or oxalate containing solutions. It suggests that the latter organic anions participate in the complex mechanism of the reduction process.

The question arises if the surface layer of the described character is present not only as a cover for the metal but as an intermediate in the cathodic deposition, so that some of the species in it may be essential for the induced deposition mechanism.

It is interesting to note that alloys of low W content do not exhibit a multiple peak ALSV, but dissolve readily through a single peak (Fig. 1c), very similar to that of pure Ni. This suggests that a substantial W content is required for the formation of the stable surface oxide layer, which hinders transport of W and Ni out from the bulk of the alloy during ALSV dissolution (Fig. 1 a and b) and provides for the different dissolution kinetics of the different phases.

Concerning the bulk of the alloy, the phase diagram for the Ni-W system¹⁰ is relevant for information about the structures which could possibly be found in the system. These are: two solid solutions, one at low (up to 20 %) and one at high W content (from 20 % to 50 %) and an intermetallic compound of the composition Ni₄W. As is known in electrochemical metal deposition, one could expect a multitude of phases to be present simultaneously in a deposit, rather than that pertaining to a given chemical composition in an equilibrated alloy. Hence, it is not unexpected that for the Ni-W alloys, selective anodic oxidation reveals the presence of several phases, from phases rich in Ni to phases rich in W. According to the ALSVs, the bulk of the electrodeposited Ni-W alloys contain up to three phases which should be assigned as follows: a solid solution of W in Ni represented by peak II, the intermetallic compound Ni₄W by peak III and a small quantity of a solid solution of W in Ni with more than 20 % W (peak IV).

The participation of different phases in the deposits and their possible prevalence depends on all the investigated process variables (on the deposition current density or deposition potential, the hydrodynamic conditions and the concentrations of species in the electrolyte). A decrease of the W content in the alloy leads to a shift of the potential of peak I in the negative direction, approaching the dissolution potential of pure Ni. The shift of the peak potential in the negative direction should be a consequence of the decrease of the WO_{2.72} and W content in the corresponding solid solutions. Simultaneously, the peaks reflecting phases rich in W (peak III and IV) disappear.

It can be seen from Table I that the efficiencies of deposition current, η , vary between 0.28 and 0.72, implying that the deposits are obtained to a quantity equivalent to 1.2 to 2.9 C cm⁻².

Only the alloys containing the above described surface layer exhibited peak III, which could be ascribed to the intermetallic compound. Prolonged deposition led to an increase of the content of the intermetallic compound in the alloy.

Corrosion of the alloy deposits

As said at the outset, the main aim of this investigation was to obtain insight into the corrosion properties of Ni-W alloys of different structures.

When the pure metals are considered in the oxygen-free acid sulfate, as a typical corrosion medium causing “hydrogen corrosion”, it can be seen from Fig. 2 that, after 120 min of open circuit stabilization, the corrosion potential (OCP) of W is some 220 mV more positive than that of electrodeposited Ni.

Inasmuch as currents obtained in the vicinity of the OCP are relevant for corrosion, measurements were extended in this work to high cathodic potentials, in order to obtain an insight into the catalytic properties of the surface for the hydrogen evolution reaction (h.e.r). It has been maintained that this is the main factor determining the hydrogen corrosion, as it controls the cathodic side of the corrosion reaction.

The obtained Tafel dependencies for pure Ni are in accordance with literature data.⁸ The cathodic slope of -120 mV dec^{-1} for hydrogen evolution as well as that of 40 mV dec^{-1} for the anodic dissolution of Ni were found as expected. Such a behavior is similar to that of iron, cobalt and zinc as stated in the literature.

The corrosion characteristics of the alloys could be compared with those of pure Ni and pure W. The alloys attain corrosion potentials in the range between those of Ni (-0.274 V vs. SCE) and W (-0.050 V vs. SCE). Also, the larger the Ni content, the closer are the corrosion potential and corrosion c.ds, j_{cor} , to that of pure Ni, and the larger is the quantity of electricity under the first peak (I), reflecting a larger proportion of Ni rich phases.

It should be noted that the corrosion c.ds, j_{cor} , were extracted from the set of passivation experiments (Fig. 5) where the measurements were taken immediately after immersion into the solution. However, from the rest of the polarization measurements, taken after 120 min of stabilization at OCP, which are relevant for the corrosion of the alloy in practice, an order of magnitude lower corrosion rates were obtained. The lowest corrosion rate was that for the alloy with some intermediate W content (10%). This alloy (sample 7) besides the surface phase, contained only one phase in the bulk, *i.e.*, a solid solution of W in Ni. The reason for such a behavior could be that after the elution of Ni from the apparently “single phase” solid solution lattice, an evenly structured alloy surface enriched in W is revealed. A homogenous surface phase composition should lead to a better corrosion resistance of these alloys, as stated by Donten and Stojek.⁴ The rate of corrosion of the alloys containing other phases (intermetallic compound and solid solution with higher W content) was one order of magnitude higher. Alloys consisting of a solid solution with low W content exhibited the highest corrosion rate. This could be a consequence of the presence, besides the solid solution of W, of some W-free pure Ni. The latter was seen to exhibit a high rate of corrosion.

According to the literature² a cathodic Tafel slope of $b_c \approx -120 \text{ mV dec}^{-1}$ is to be expected for pure W in a H_2SO_4 solution after removing oxides, as well as for WO_3/Pt . However, in the present case (Fig. 2), different slopes were recorded and the entire cathodic polarization behavior resembles that of tungsten bronzes.¹¹ Hydrogen tungsten bronzes are nonstoichiometric mixed oxides of general formula $\text{A}_{1-x}\text{M}_y\text{O}_z$; where M is a transition metal, M_yO_z its binary oxide and A is some other metal or hydrogen. The formation of blue hydrogen tungsten bronzes occurs whenever WO_3 is exposed to reducing conditions. Similar colors are found in the deposits of the Ni-W alloys. Bronze oxides are known to be chemically inert, metallic conductors. H-compounds are typical

group members, except that they are sensitive towards oxidizing conditions under which they are reconverted to the parent oxide.

The cathodic polarization of W bronzes is characterized by the appearance of a limiting current of 20–50 $\mu\text{A cm}^{-2}$, at low polarizations. At larger polarizations, two Tafel slopes of –120 and –180 mV dec^{-1} are to be expected. The change from one slope to the other was explained by a change in the electrode coverage with hydrogen. Upon cathodic polarization in the reverse direction, a limiting current was not recorded. Instead, in that potential range, a linear dependence was obtained with slopes ranging from –40 to –120 mV dec^{-1} , depending on the sweep rate. In the range where a limiting current was noted, *i.e.* at low polarizations, from OCP up to the reversible potential of the h.e.r., a reduction of hydrated non-stoichiometric oxides is likely to occur.

Similar behavior was found here with the Ni-W alloys: the cathodic polarization of the alloys, at potentials more positive than the reversible potential of hydrogen, exhibit a limiting current of the order of 10 $\mu\text{A cm}^{-2}$. At alloys rich in Ni, as the corrosion potential shifts in a negative direction, the limiting current becomes less pronounced. The rate of the h.e.r. at alloys at one and the same potential is up to ten times larger than at pure Ni, reflecting the increasing catalytic effect of W oxides, which was noted elsewhere.¹¹ Ageing of the alloys produces similar effects (Fig. 4), reflecting the elution of Ni and the increasing participation of bronzelike W-oxides. The longer the ageing, the more pronounced is the effect.

Passivation phenomena

Both Ni and W are metals known to undergo passivation in most electrolytes reflecting a build-up of tough, non-porous films of different nature. Hence, a similar phenomenon was expected to occur with the deposited Ni-W alloys. Hence, ALSV was run in an acid sulfate electrolyte from the OCP up to highly positive potentials, passed 1.5 V *vs.* SCE. As can be seen in Fig. 5, pure Ni actively dissolves with two peaks in the voltammogram, up to a potential of about 0.2 V *vs.* SCE, when it suddenly passivates with the c.d. falling by several orders of magnitude, to values around 1 $\mu\text{A cm}^{-2}$. The transpassive region starts at potentials in excess of 1 V *vs.* SCE. Hence, a large potential window exists in which Ni is virtually completely protected from corrosion.

Pure W passivates virtually from the OCP and stays passive till the positive potential limit, with a dissolution c.d. around 20 $\mu\text{A cm}^{-2}$. The alloys exhibit different behavior. Only the one with the low W-content (3 %) exhibited behavior similar to that of pure Ni. Hence, obviously, that amount of W in the solid solution could not affect the formation of the passive Ni-oxide film. In these two cases, the rate of corrosion was rather large in the active potential region (*cf.* Table II). Yet, in both cases passivation occurs already at reasonably low anodic potentials. Thus, in most practical applications, when oxygen is amply present in the atmosphere, the OCP is likely to be in the passive region of potentials (oxygen corrosion) and the deposit should be well protected against corrosion.

On the contrary, alloys with a larger W-content are seen to maintain relatively large dissolution c.d. all the way to positive limit of potential much larger than those at pure W. Although the dissolution currents are virtually constant and independent of po-

tential in that region, resembling passive behavior, they are so large that the deposit cannot be considered as being protected against corrosion by passivity. This suggests that mixtures of W and Ni are not suitable for building passive film structures. However, this group of alloys with relatively high W contents is superior to pure Ni or low-W content alloys, when the conditions of the corrosive medium set the corrosion potential between the OCP of the former and the OCP of the latter.

CONCLUSIONS

On the basis of ALSV analysis, literature data and phase diagram for Ni-W alloys, it could be concluded that the bulk electrochemically deposited alloys may consist of three different phases, all of them present simultaneously in high W-content alloys, which are: a solid solution of W in a nickel matrix (up to 20 mol % W); the intermetallic compound Ni₄W and an over saturated solid solution of W in nickel (over 20 mol % W).

As revealed by XPS analysis, the electrodeposited Ni-W alloys of high W-content are covered with a surface layer of complex structure and composition. Apart from pure Ni and W, it contains: Ni(OH)₂ and WO₃, on the very surface. In the layer immediately beneath, some reduced oxide of the composition WO_{2.72} (*i.e.*, a solid solution of WO_{2.72} in nickel) and some tungsten carbide were also found.

It appears that the former layer is present at the surface during induced cathodic deposition, as well as during the corrosion process. It is highly likely that some of the oxide species in the layer also act as an intermediate in the deposition process. Identifying those species should give a clue to a more detailed understanding of the mechanism of induced deposition of W than has been achieved so far.

Corrosion of the investigated Ni-W alloys in acid solution at OCP occurs by a preferential dissolution of nickel from the surface layer. Subsequently, as the corrosion process proceeds, the polarization characteristics indicate that the surface behaves as one of pure tungsten. The lowest initial corrosion rates were recorded with alloys rich in W. The larger the W content, the lower are the corrosion c.d.s, approaching that of pure W. After ageing at OCP, the lowest corrosion c.d. was found for the alloy consisting of a solid solution only.

An important conclusion could be made based on the results of the present investigations: In the absence of oxygen or some other depolarizer rendering a highly positive OCP, the corrosion resistance of the high-W-content alloys are superior to that of pure Ni or low-W-content alloys. On the contrary, high-W alloys offer poor corrosion resistance in the presence of oxygen, at least until Ni is dissolved from the surface.

ИЗВОД

КАРАКТЕРИЗАЦИЈА И КОРОЗИОНЕ КАРАКТЕРИСТИКЕ ЕЛЕКТРОХЕМИЈСКИ ТАЛОЖЕНЕ ЛЕГУРЕ Ni-W

М. ОБРАДОВИЋ¹, Ј. СТЕВАНОВИЋ¹, А. ДЕСПИЋ¹, Р. СТЕВАНОВИЋ¹ и Ј. СТОСН²¹ИХТМ - Центар за електрохемију, Њеџошева 12, б. бр. 473, 11001 Београд, Југославија (e-mail: rade@elab.tmf.bg.ac.yu) и ²Institute of Catalysis and Surface Chemistry, Polish Academy of Sciences, Niezapominajek 1, 30-239 Krakow, Poland

Електрохемијски таложене легуре Ni-W из цитратног раствора садрже три различите фазе, које су присутне при високом садржају W у легури: чврст раствор W у Ni; интерметално једињење Ni₄W и чврст раствор W у Ni са садржајем W већим од 20 mol %. XPS анализом је показано да су легуре покривене слојем сложене структуре. Овај слој садржи чисте метале Ni и W, Ni(OH)₂ и WO₃, на самој површини. У слоју испод саме површине нађени су и делимично редукован оксид WO_{2,72} (највероватније чврст раствор WO_{2,72} у Ni) и волфрам-карбид. Врло је вероватно да нека од оксидних врста у слоју учествује као интермедијер у процесу катодног таложјења. Идентификација те врсте могла би допринети бољем разумевању механизма индукованог таложјења волфрама. На потенцијалу отвореног кола у сумпорној киселини корозиони процес се одиграва тако што се преференцијално раствара Ni из површинског слоја легуре. Уколико корозиони процес траје дуже утолико корозионе карактеристике постају све сличније онима за чист W. Ниже почетне брзине корозије добијене су за легуре са већим садржајем W. Међутим, након стајања на потенцијалу отвореног кола ниже корозионе струје су добијене за Ni-W легуру хомогене фазне структуре која садржи само чврст раствор.

(Примљено 30 јула, ревидирано 8. августа 2001)

REFERENCES

1. A. Brenner, *Electrodeposition of Alloys, Principles and Practice*, Academic Press, New York, (1963)
2. A. T. Vasko, *Elektrohimiya volframa*, I Tekhnika, Kiev (1969)
3. N. Atanasov, K. Gencheva, M. Bratoeva, *Plating & Surface Finishing* **84** (1997) 67
4. M. Donten, Z. Stojek, *J. Appl. Electrochem.* **26** (1996) 665
5. M. Obradović, J. Stevanović, A. Despić, R. Stevanović, *J. Serb. Chem. Soc.* **64** (1999) 245
6. A. R. Despić, V. D. Jović, in *Modern Aspects of Electrochemistry*, Vol 27, R. E. White, J. O'M. Bockris and B. E. Conway, Eds., Plenum Press, New York (1995)
7. V. V. Bondar, V. V. Grinina, V. N. Pavlov, *Elektroosazhdenie dvoinyh splavov*, Itogi Nauki i Tehniki, Moscow (1970)
8. D. M. Dražić, V. Vaščić, *J. Electroanal. Chem.* **185** (1985) 229
9. M. Donten, Z. Stojek, *51st ISE Meeting*, Abstract 894-8-P, Warsaw, Poland, 2000
10. P. Gustafson, *Calphad* **11** (1987) 277
11. D. B. Šepa, D. S. Ovcin, M. V. Vojnović, *J. Electrochem. Soc.* **119** (1972) 1285.